

LETTER TO THE EDITOR

## Late-time emission of type Ia supernovae: optical and near-infrared observations of SN 2001el <sup>★,★★</sup>

M. Stritzinger<sup>1</sup> and J. Sollerman<sup>1,2</sup>

<sup>1</sup> Dark Cosmology Centre, Niels Bohr Institute, University of Copenhagen, Juliane Maries Vej 30, 2100 Copenhagen Ø, Denmark  
e-mail: [max, jesper]@dark-cosmology.dk

<sup>2</sup> Stockholm Observatory, AlbaNova, Department of Astronomy, 106 91 Stockholm, Sweden

Received 21 December 2006 / Accepted 6 May 2007

### ABSTRACT

**Aims.** To elucidate the nature of the late-phase emission of the normal type Ia supernova SN 2001el.

**Methods.** We present optical and near-infrared light curves of SN 2001el from 310 to 445 days past maximum light, obtained with the Very Large Telescope.

**Results.** The late-time optical (*UBVRI*) light curves decay in a nearly linear fashion with decay time scales of  $1.43 \pm 0.14$ ,  $1.43 \pm 0.06$ ,  $1.48 \pm 0.06$ ,  $1.45 \pm 0.07$ , and  $1.03 \pm 0.07$  magnitudes (per hundred days) in the *U*, *B*, *V*, *R*, and *I* bands, respectively. In contrast, in the near-infrared (*JHK<sub>s</sub>*) bands the time evolution of the flux appears to be nearly constant at these epochs. We measure decline rates (per hundred days) of  $0.19 \pm 0.10$  and  $0.17 \pm 0.11$  magnitudes in the *J* and *H* bands, respectively. We construct a UVOIR light curve, and find that the late-time luminosity has a decay time scale nearly consistent with complete deposition of positron kinetic energy.

**Conclusions.** The late-time light curves of the normal type Ia SN 2001el demonstrate the increased importance of the near-infrared contribution. This was previously observed in the peculiar SN 2000cx, and the results for SN 2001el thus ensure that the conclusions previously based on a single peculiar event are applicable to normal type Ia supernovae. The measured late-time UVOIR decline rate suggests that a majority of the positrons are trapped within the ejecta. This result does not favor the prediction of a weak and/or radially combed magnetic field configuration.

**Key words.** stars: supernovae: general – stars: supernovae: individual: SN 2001el

### 1. Introduction

Type Ia supernovae (hereafter SNe Ia) are an exceptionally useful tool for cosmological investigations (see e.g. Leibundgut 2001, and references therein). A large observational data set has been assembled, and major theoretical efforts have led towards an understanding of these stellar explosions. However, most of the observational and theoretical focus has been directed towards the understanding of SNe Ia during the early photospheric phase. The study of the late-phases of thermonuclear supernovae, on the other hand, offers other opportunities to study the physics of these explosions.

At times greater than  $\sim 150$  days past maximum light, the ejecta are transparent to the majority of  $\gamma$  rays originating from the decay of the radioactive isotopes synthesized in the explosion. The light curves are then powered by the deposition of positron kinetic energy. The fraction of positron energy that is deposited into the ejecta is thought to depend on the configuration of the magnetic field; a strong and tangled magnetic field should trap a majority of positrons whilst a weak and radially combed field would lead to a large positron escape fraction.

Late-time light curves therefore provide a way to understand the magnetic field structure (Colgate et al. 1980; Ruiz-Lapuente & Spruit 1998; Milne et al. 1999, 2001). If positrons are trapped

(escape), a flattening (steepening) in the bolometric light curve is expected. With this knowledge it should then be possible, at least in principle, to constrain the contribution these positrons make to the Galactic 511 KeV line.

The late-phases also allow for the study of other important aspects of the physics of SNe Ia, such as the nucleosynthesis of radioactive (Stritzinger et al. 2006) and stable (Kozma et al. 2005) elements, as well as the distribution of these elements (e.g. Motohara et al. 2006). In addition, the late-phases allow us to probe the physics of freeze-out and of the infrared catastrophe (Axelrod 1980; Fransson et al. 1996; Sollerman et al. 2004).

Early investigations proposed evidence for varying degrees of trapping (Cappellaro et al. 1997; Ruiz-Lapuente & Spruit 1998; Milne et al. 1999, 2001). However, all such studies of the late-time emission were limited due to a lack of late-time near-infrared data (but see Elias & Frogel 1983).

A pioneering investigation of the optical and near-infrared late-time flux evolution of SN 2000cx found evidence for a less steep decrease of the bolometric light curve due to the increasing importance of the near-infrared contribution (Sollerman et al. 2004). Although these findings for SN 2000cx were interesting for our understanding of positron trapping and the physics of the late-phases, it was noted that SN 2000cx was peculiar at early times (Li et al. 2001; Candia et al. 2003). A concern was thus that its late-phase behaviour may have been atypical compared to normal SNe Ia. Here we conduct a similar study for a normal and more representative SN Ia.

\* Based on observations collected at the European Southern Observatory, Paranal, Chile (ESO Programmes 69.D-0193(ABCD) and 70.D-0023(AB)).

\*\* Tables 1–4 are only available in electronic form at <http://www.aanda.org>

**Table 5.** Late-time optical magnitudes of SN 2001el.

Phase <sup>a</sup> (days)	<i>U</i>	<i>B</i>	<i>V</i>	<i>R</i>	<i>I</i>
310	21.64(0.09) <sup>b</sup>	20.22(0.05)	20.04(0.05)	20.45(0.06)	19.68(0.05)
367	...	...	20.88(0.10)	21.16(0.09)	20.17(0.10)
370	...	...	20.95(0.04)	21.36(0.04)	20.28(0.03)
398	22.81(0.14)	21.45(0.06)	...	...	...
430	23.44(0.25)	...	21.81(0.06)	22.25(0.16)	...
436	...	22.03(0.07)	...	22.61(0.15)	20.99(0.08)
437	23.56(0.31)	...	...	22.18(0.08)	...

<sup>a</sup> Refers to days past  $B_{\max}$ .

<sup>b</sup> Numbers in parentheses are uncertainties.

### 1.1. SN 2001el

SN 2001el was discovered on 17 September 2001 (UT) (Monard 2001) in the nearby spiral galaxy NGC 1448. NED gives a redshift to this galaxy of  $1168 \text{ km s}^{-1}$ . The supernova was located  $18''$  west and  $20''$  north of the nucleus. Four days after discovery, Sollerman et al. (2001) classified it as a bona fide SN Ia. This supernova has been targeted by several groups and a number of papers are now available. Early-phase light curves presented by Krisciunas et al. (2003) indicate SN 2001el to be a normal event with a  $\Delta m_{15}(B) = 1.13 \pm 0.04$  mag. The time of *B*-band maximum was JD 2452 182.5 or 30 September 2001. Sollerman et al. (2005) estimated the host galaxy extinction to be  $E(B - V)_{\text{host}} = 0.18 \pm 0.08$  mag, and the dust maps of Schlegel et al. (1998) list the Galactic component to be  $E(B - V)_{\text{gal}} = 0.014$  mag. Mattila et al. (2005) published early- and late-time spectroscopy obtained with the Very Large Telescope (VLT).

We selected SN 2001el for a VLT study since it was nearby, well-studied at early phases, and located in a favorable position within the host galaxy. The sky position allowed a dedicated multi-epoch multi-band observational campaign to be conducted at the VLT. In this letter we present these late-time optical and near-infrared photometric observations of SN 2001el.

## 2. Observations and data analysis

### 2.1. Optical imaging with the VLT

Late-time multi-epoch *UBVRI*-band observations of SN 2001el were obtained with the FOCal Reducer and low dispersion Spectrograph (FORS1) attached to UT1 (Aug.–Oct. 2002) and UT3 (Nov.–Dec. 2002) of the VLT. Service mode imaging was conducted from 310 to 437 days past *B*-band maximum. Table 1 contains a log of the optical observations.

FORS1 uses a  $2048 \times 2048$  pixel sized charged coupled device with a pixel scale of  $0''.20$  per pixel. To obtain an adequate signal-to-noise while preventing saturation of field stars, multiple exposures were obtained in each filter. All frames were bias-subtracted and twilight-sky flattened using MIDAS. Frames taken for a given night with the same filter were then combined with IRAF<sup>1</sup> scripts.

The brightness of SN 2001el was determined differentially with respect to a sequence of local field stars. Absolute photometry of the local sequence was obtained using standard stars in the fields Mark A and PG 41528+062 (Landolt 1992), which

were observed under photometric conditions on 5 August 2002. Instrumental magnitudes of the standard fields were computed using the IRAF DAOPHOT package `phot` with an aperture radius of  $7''$ . The instrumental magnitudes were then used to derive the zero-points used to put the local sequence on the standard system.

Instrumental magnitudes of 10 stars in the local field were computed using `phot` with an aperture radius of  $0''.5$ . Aperture corrections were then computed using the IRAF task `mkapfile`. The instrumental magnitudes were corrected for color term and atmospheric absorption and then put on the standard system using the zero-points computed from the Landolt fields. Table 2 lists their standard magnitudes, where the listed uncertainties include errors associated with the photometric zero-point and the errors computed by `phot` and `mkapfile`. Note that in the *U* band only 8 of the sequence stars are bright enough to calculate an accurate magnitude. These local sequence stars showed a night-to-night dispersion of less than  $0.05$  mag (std. dev.) over the entire duration of the programme.

Instrumental magnitudes of the supernova were measured using `phot` with an aperture radius of  $0''.5$ . When using the Landolt standards to solve for the photometric solutions we found that the color terms and extinction coefficients were very similar to the averaged values provided on the ESO web-page<sup>2</sup>. As the ESO values are based on a significantly larger number of standard stars we decided to adopt these averaged values. This allowed us to reduce the number of fitting parameters such that it was only necessary to compute the zero-point for each epoch using the local sequence.

Table 5 contains the *UBVRI*-band photometry of SN 2001el. The quoted uncertainties were calculated by adding in quadrature the errors associated with the nightly zero-point, and the errors computed by `phot` and `mkapfile`.

### 2.2. Infrared observations with the VLT

Late-time multi-epoch *JHK<sub>s</sub>*-band observations were obtained with the Infrared Spectrometer And Array Camera (ISAAC)<sup>3</sup> attached to UT1 of the VLT. ISAAC is equipped with a  $1024 \times 1024$  pixel sized Rockwell Hawaii HgCdTe detector with a pixel scale of  $0''.147$  per pixel and a  $2'.5 \times 2'.5$  field of view. Imaging was conducted in the short wavelength mode from 316 to 445 days past maximum light. A log of the observations is given in Table 3.

<sup>1</sup> The Image Reduction and Analysis Facility (IRAF) is maintained and distributed by the Association of Universities for Research in Astronomy, under a cooperative agreement with the National Science Foundation.

<sup>2</sup> [http://www.eso.org/observing/dfo/quality/index\\_fors1.html](http://www.eso.org/observing/dfo/quality/index_fors1.html)

<sup>3</sup> <http://www.eso.org/instruments/isaac/>

**Table 6.** Late-time near-infrared magnitudes of SN 2001el.

Phase <sup>a</sup> (days)	<i>J</i>	<i>H</i>	<i>K<sub>s</sub></i>
316	...	18.40(0.12) <sup>b</sup>	20.07(0.21)
317	19.15(0.10)	...	...
370	19.21(0.11)	18.62(0.11)	19.36(0.42)
383	...	...	19.54(0.52)
443	19.55(0.12)	18.89(0.11)	...
445	19.23(0.12)	18.47(0.12)	...

<sup>a</sup> Refers to days past  $B_{\max}$ .<sup>b</sup> Numbers in parentheses are uncertainties.

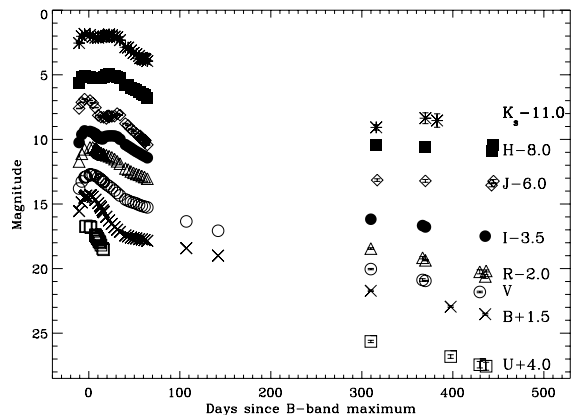
As SN 2001el was fairly close to the galaxy, imaging was performed using the jitter–offset method. The procedure typically consists of obtaining two images of the galaxy with a small offset of the telescope between each frame. The telescope is then dithered off source to obtain an image of the sky. Multiple iterations of jitter–offset are performed and a data cube for each filter is obtained.

All data were reduced using the Eclipse<sup>4</sup> software package. The task `jitter` was used to estimate and remove the sky background, and then combine each on-source image within the data cube.

A local sequence consisting of 7 stars in the field around NGC 1448 was calibrated with standard fields. Instrumental magnitudes of the standard stars were obtained using `phot` with an aperture radius of  $0''.5$  and aperture corrections were then computed with `mkapfile`. In the *J* band the local sequence was calibrated using the standard fields FS31 and FS32 (Hawarden et al. 2001; Leggett et al. 2006), which were observed on 17 December 2002, while observations of the standard star field FS19 obtained on 16 December 2002 was used to calibrate the local sequence in the *H* band. Three of our local sequence stars were observed by the 2MASS all-sky survey. We found that our calibrated *JH*-band magnitudes of the 2 brightest of these 3 stars agreed with the 2MASS value to within 0.1 mag. For the *K<sub>s</sub>* band we were unable to obtain a zero-point from the observed standard fields that gave magnitudes consistent with the 2MASS observations. We therefore calibrated the local sequence in the *K<sub>s</sub>* band using the two bright sequence stars that are in common with the 2MASS catalog.

Magnitudes of the photometric sequence (corrected for atmospheric extinction<sup>5</sup>) are listed in Table 4. No color term corrections were applied. The quoted uncertainties are added in quadrature using the errors in the zero-points, and the errors computed by `phot` and `mkapfile`. We found the night-to-night dispersion of each sequence star over the course of the programme to be less than 0.05 mag (std. dev.).

Aperture photometry of the supernova was computed with `phot` using an aperture radius of  $0''.5$  and then aperture corrected. Table 6 lists the *JHK<sub>s</sub>*-band photometry. The quoted uncertainties were determined by adding in quadrature the errors associated with the nightly zero-point, the photometric error computed by `phot`, the error computed by `mkapfile`, and a 0.10 magnitude error (for *JH* bands) associated with the difference between our standard magnitudes and the 2MASS magnitudes.

**Fig. 1.** *UBVR IJHK<sub>s</sub>* light curves of SN 2001el plotted as a function of time since *B*-band maximum. Early-time photometry (<200 days) is from Krisciunas et al. (2003). The data have been shifted in the *y*-direction for clarity as indicated.

### 3. Results

In Fig. 1 we present optical and near-infrared light curves of SN 2001el. Here the early-time data from Krisciunas et al. (2003) are plotted together with our late-time (>300 days past  $B_{\max}$ ) VLT photometry. No extinction corrections have been applied to these light curves. As seen in Fig. 1 the late-time optical light curves follow a nearly linear decline, while the near-infrared light curves are essentially flat. We measure decline rates (mag per hundred days) of  $\approx 1.45$  for the *UBVR* light curves, a shallower 1.03 in the *I* band,  $\approx 0.20$  in the *J* and *H* bands, and  $\approx -1.0 \pm 0.7$  in the *K<sub>s</sub>* band. Table 7 lists the exact late-time decline rates for all passbands. A final *K<sub>s</sub>*-band image was obtained 443 days past maximum light. However, the final sky-subtracted image was not deep enough to provide any intensity limit on the supernova brightness at this epoch.

We constructed an UltraViolet Optical near-InfraRed (UVOIR) bolometric light curve following the method of Contardo et al. (2000); see Fig. 2. To place the UVOIR flux on an absolute flux scale we adopted the extinction given in Sect. 1.1 and a distance to NGC 1448 of 17.9 Mpc (Mattila et al. 2005).

With the late-phase UVOIR light curve we can estimate the fraction of flux (as a function of time) emitted in the *JHK<sub>s</sub>* passbands. It is found that the percentage of UVOIR flux in these passbands during 310 to 445 days past maximum light increases from  $\sim 6\%$  to  $\sim 25\%$ .

A least-squares fit to the late-time UVOIR light curve yields a decline rate (per hundred days) of 0.90 mag. This is consistent with the 0.98 mag decline rate expected for the case of complete deposition of positron kinetic energy.

Finally, to estimate the  $^{56}\text{Ni}$  mass we performed a least-squares fit of a radioactive decay energy deposition function for the  $^{56}\text{Co} \rightarrow ^{56}\text{Fe}$  decay chain to our UVOIR light curve between 50 and 450 days past maximum brightness. The functional form of the toy model used (see Sollerman, Leibundgut & Spyromilio 1998) is  $L = 1.3 \times 10^{43} M_{\text{Ni}} e^{-t/111.3} (1 - 0.966e^{-\tau})$ , in units of  $\text{erg s}^{-1}$ , where the optical depth,  $\tau$ , is given by  $(t_1/t)^2$ . In this case  $t_1$  sets the time when the optical depth to  $\gamma$  rays is unity. We find that a best fit to the data is obtained with a  $t_1$  of 35 days and a  $^{56}\text{Ni}$  mass of  $0.40 M_{\odot}$  (see Fig. 2).

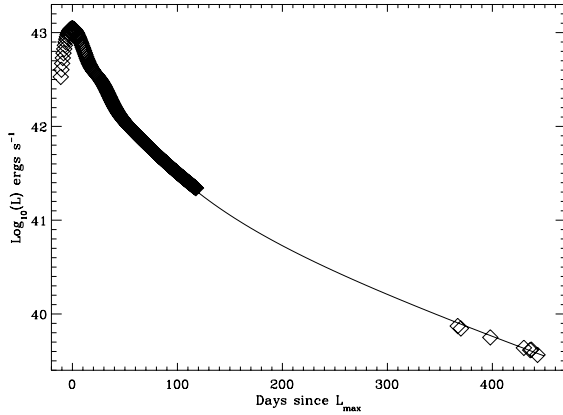
By comparing this  $^{56}\text{Ni}$  mass to the estimate presented by Stritzinger et al. (2006) (corrected to the same absolute flux scale used in this work), which used Arnett’s rule, we can constrain the amount of flux not encapsulated in our late-time UVOIR

<sup>4</sup> <http://www.eso.org/projects/aot/eclipse/><sup>5</sup> The photometry was corrected for atmospheric absorption using standard extinction coefficients: [http://www.eso.org/instruments/isaac/imaging\\_standards.html](http://www.eso.org/instruments/isaac/imaging_standards.html)

**Table 7.** Decline rates of late-time light curves<sup>a</sup>.

<i>U</i>	<i>B</i>	<i>V</i>	<i>R</i>	<i>I</i>	<i>J</i>	<i>H</i>	<i>K<sub>s</sub></i>
1.43(0.14)	1.43(0.06)	1.48(0.06)	1.45(0.07)	1.03(0.07)	0.19(0.10)	0.17(0.11)	-1.04(0.65)

<sup>a</sup> Mag per 100 days between 310 and 450 days; errors in parenthesis are  $1\sigma$ .

**Fig. 2.** The UVOIR light curve (diamonds) fitted with our toy model (full line).

light curve. We find that  $\sim 40\%$  of the total flux is emitted outside the covered passbands. This value is consistent with results obtained from both observations and modeling of SN 2000cx (Sollerman et al. 2004). It must be noted however that our toy model, Arnett’s rule, and the modeling of SN 2000cx are all based on a number of uncertain assumptions, so these results should only be considered as indicative. It is important to keep in mind that we are still not probing the true bolometric light curve.

#### 4. Discussion

This is the first normal SN Ia for which we have systematically monitored the late-time light curves in both the optical and the near-infrared. The optical late-time behaviour of SN 2001el is nearly identical to that of other SNe Ia that have been studied at late-phases. The *BVRI*-band decline rates are in agreement with the average decline rates presented by Milne et al. (2001) and Lair et al. (2006) for a number of normal SNe Ia. Our *U*-band light curve shows a decline rate similar to that of the other optical bands (but see Stanishev et al. 2007).

The shallow decline in the *I* band suggests a shift of flux towards the near-infrared, as also indicated by Sollerman et al. (2004) and Lair et al. (2006). This is confirmed by our late *JHK<sub>s</sub>* light curves. After  $\sim 300$  days past maximum light the emission redward of 1.1 microns becomes increasingly important. This behaviour was documented with the detailed observations of SN 2000cx (Sollerman et al. 2004). Our observations of SN 2001el indicate that at late-phases SN 2000cx behaved like a *normal* SN Ia. Similar behaviour was seen with limited near-infrared observations of three other normal SNe Ia: SN 1998bu (Spyromilio et al. 2004), SN 2003cg (Elias-Rosa et al. 2006), and SN 2004S (Krisciunas et al. 2007).

The decline rate of the late-time UVOIR light curve indicates that few positrons escape the ejecta. This result does not

favor predictions of a weak and/or radially combed magnetic field configuration.

We have presented modeling of the late-phase observations of SN 2000cx and we refer the reader to Sollerman et al. (2004) for a general discussion concerning the physics driving these observations. The main result of the current paper is the demonstration that the increasing importance of the late-time near-infrared light curves is indeed a generic feature of normal SNe Ia. This result challenges the assumption used by other studies that the late-time bolometric light curve follows the optical light curves. Therefore any conclusions regarding positron escape and their contribution to the Galactic 511 KeV line which had hitherto been based on optical photometry alone must be reevaluated. These data will serve as sorely needed input for modeling that will attempt to address this issue.

*Acknowledgements.* The Dark Cosmology Centre is funded by the Danish National Research Foundation. This research was supported in part by the National Science Foundation under Grant No. NSF PHY05-51164. Special thanks to the referee for a prompt and useful report. We thank Johan Fynbo and Pall Jakobsson for helpful discussions on data reductions, and also Bruno Leibundgut, Peter Lundqvist, Kevin Krisciunas, Peter Milne, and Dong Xu for discussions related to this project. This research has made use of the Two Micron All-Sky Survey, and the NASA/IPAC Extragalactic Database (NED), which is operated by the Jet Propulsion Laboratory, California Institute of Technology, under contract with the National Aeronautics and Space Administration.

#### References

- Axelrod, T. S. 1980, Ph.D. Thesis, Univ. of California, Santa Cruz  
 Candia, P., Krisciunas, K., Suntzeff, N. B., et al. 2003, *PASP*, 115, 277  
 Cappellaro, E., Mazzali, P. A., Benetti, S., et al. 1997, *A&A*, 329, 203  
 Colgate, S. A., Petscheck, A. G., & Kriese, J. T. 1980, *ApJ*, 237, L81  
 Contardo, G., Leibundgut, B., & Vacca, W. D. 2000, *A&A*, 359, 876  
 Elias, J. H., & Frogel, J. A. 1983, *ApJ*, 268, 718  
 Elias-Rosa, N., Benetti, S., Cappellaro, E., et al. 2006, *MNRAS*, 369, 1880  
 Fransson, C., Houck, J., & Kozma, C. 1996, *Supernovae and Supernova Remnants*, IAU Coll., 145, 211  
 Hawarden, T. G., Leggett, S. K., Letaqsky, M. B., et al. 2001, *MNRAS*, 325, 563  
 Kozma, C., Fransson, C., Hillebrandt, W., et al. 2005, *A&A*, 437, 983  
 Krisciunas, K., Suntzeff, N. B., Candia, P., et al. 2003, *AJ*, 125, 166  
 Krisciunas, K., Garnavich, P., Suntzeff, N. B., et al. 2007, *AJ*, 133, 58  
 Lair, J., Leising, M. D., Milne, P., et al. 2006, *AJ*, 132, 2024  
 Landolt, A. U. 1992, *AJ*, 104, 340  
 Li, W., Filippenko, A. V., Gates, E., et al. 2001, *PASP*, 113, 1178  
 Leibundgut, B. 2001, *A&A Rev.*, 39, 67  
 Leggett, S. K., Currie, M. J., Varricatt, W. P., et al. 2006, *MNRAS*, 373, 781  
 Mattila, S., Lundqvist, P., Sollerman, J., et al. 2005, *A&A*, 443, 649  
 Milne, P. A., The, L. S., & Leising, D. 1999, *ApJS*, 124, 503  
 Milne, P. A., The, L. S., & Leising, D. 2001, *ApJ*, 559, 1019  
 Monard, A. G. 2001, *IAU Circ.*, 7720  
 Motohara, K., Maeda, M., Gerardy, C. L., et al. 2006, *ApJ*, 652, 101  
 Ruiz-Lapuente, P., & Spruit, H. 1998, *ApJ*, 500, 360  
 Schlegel, D. J., Finkbeiner, D. P., & Davis, M. 1998, *ApJ*, 500, 525  
 Sollerman, J., Leibundgut, B., & Spyromilio, J. 1998, *A&A*, 337, 207  
 Sollerman, J., Leibundgut, B., & Lundqvist, P. 2001, *IAU Circ.*, 7723  
 Sollerman, J., Lindahl, J., Kozma, C., et al. 2004, *A&A*, 428, 555  
 Sollerman, J., Cox, N., Mattila, S., et al. 2005, *A&A*, 429, 559  
 Spyromilio, J., Gilmozzi, R., Sollerman, J., et al. 2004, *A&A*, 426, 547  
 Stanishev, V., Goobar, A., Benetti, S., et al. 2007, *A&A*, 469, 645  
 Stritzinger, M. D., Mazzali, P. A., Sollerman, J., & Benetti, S. 2006, *A&A*, 460, 793

# Online Material

**Table 1.** Log of optical VLT observations for SN 2001el.

Phase <sup>a</sup> (days)	Filter	Exposure (s)	Airmass	Seeing (arcsec)
310	<i>U</i>	2 × 800	1.24	0.89
310	<i>B</i>	3 × 180	1.41	0.56
310	<i>V</i>	3 × 150	1.32	0.62
310	<i>R</i>	3 × 150	1.28	0.66
310	<i>I</i>	3 × 180	1.25	0.56
367	<i>V</i>	3 × 300	1.23	1.16
367	<i>R</i>	3 × 300	1.19	0.98
367	<i>I</i>	3 × 300	1.15	1.08
370	<i>V</i>	3 × 300	1.08	0.60
370	<i>R</i>	3 × 300	1.19	0.60
370	<i>I</i>	3 × 300	1.11	0.60
398	<i>U</i>	2 × 1020	1.36	1.00
398	<i>B</i>	3 × 300	1.26	0.78
430	<i>U</i>	1 × 790	1.07	1.02
430	<i>V</i>	3 × 600	1.11	0.80
430	<i>R</i>	3 × 720	1.25	1.00
436	<i>B</i>	3 × 600	1.07	0.84
436	<i>R</i>	3 × 720	1.07	1.20
436	<i>I</i>	6 × 900	1.19	1.00
437	<i>U</i>	3 × 1020	1.20	1.00
437	<i>R</i>	3 × 720	1.11	0.80

<sup>a</sup> Refers to days past  $B_{\max}$ .

**Table 2.** Magnitudes for local standards in the optical.

Offsets <sup>a</sup>		<i>U</i>	<i>B</i>	<i>V</i>	<i>R</i>	<i>I</i>
181.6 N	72.8 E	20.50(0.08) <sup>b</sup>	20.68(0.05)	20.13(0.05)	19.78(0.06)	19.43(0.05)
193.6 N	61.6 E	19.84(0.08)	19.84(0.05)	19.18(0.05)	18.77(0.06)	18.40(0.05)
179.2 N	56.8 W	20.66(0.08)	20.66(0.05)	20.00(0.05)	19.59(0.06)	19.21(0.05)
6.4 N	113.6 W	20.42(0.08)	20.33(0.05)	19.61(0.05)	19.19(0.06)	18.80(0.05)
56.8 S	99.2 W	22.44(0.09)	21.41(0.05)	19.73(0.05)	18.70(0.06)	17.60(0.05)
62.4 S	95.2 W	22.73(0.10)	22.69(0.05)	22.01(0.05)	21.66(0.06)	21.32(0.06)
72.8 S	140.0 W	19.51(0.08)	19.67(0.05)	19.18(0.05)	18.86(0.06)	18.54(0.05)
73.6 N	181.6 E	20.73(0.08)	21.10(0.05)	21.02(0.05)	20.92(0.06)	20.71(0.05)
39.2 S	136.8 E	...	21.57(0.05)	20.09(0.05)	19.19(0.06)	18.33(0.05)
132.0 S	22.4 W	...	23.18(0.05)	21.62(0.05)	20.67(0.06)	19.68(0.05)

<sup>a</sup> Offsets in arcseconds measured from the supernova.

<sup>b</sup> Numbers in parentheses are uncertainties.

**Table 3.** Log of near-infrared VLT observations for SN 2001el.

Phase <sup>a</sup> (days)	Filter	Exposure <sup>b</sup> (s)	Airmass	Seeing (arcsec)
316	<i>H</i>	10 × 6 × 25	1.13	0.49
316	<i>K<sub>s</sub></i>	10 × 6 × 28	1.30	0.41
317	<i>J</i>	30 × 4 × 24	1.18	0.52
370	<i>J</i>	30 × 4 × 23	1.06	0.65
370	<i>H</i>	10 × 6 × 17	1.15	0.44
370	<i>K<sub>s</sub></i>	10 × 6 × 30	1.08	0.40
383	<i>K<sub>s</sub></i>	10 × 6 × 20	1.11	0.40
443	<i>H</i>	10 × 6 × 30	1.14	0.40
443	<i>J</i>	30 × 4 × 30	1.14	0.40
443	<i>K<sub>s</sub></i>	30 × 4 × 27	1.09	0.60
445	<i>J</i>	30 × 4 × 23	1.17	0.70
445	<i>H</i>	10 × 6 × 60	1.06	0.55

<sup>a</sup> Refers to days past  $B_{\max}$ .<sup>b</sup> Detector integration time (DIT) × number of DITs per exposure × number of exposures.**Table 4.** Magnitudes for local standards in the near-infrared.

Offsets <sup>a</sup>		<i>J</i>	<i>H</i>	<i>K<sub>s</sub></i>
55.35 N	11.96 W	12.98(0.06) <sup>b</sup>	12.57(0.05)	12.51(0.05)
41.9 N	21.4 W	17.54(0.06)	16.89(0.05)	16.09(0.05)
17.4 S	46.3 W	13.56(0.06)	13.18(0.05)	13.07(0.05)
25.4 S	42.3 E	17.54(0.06)	17.24(0.05)	16.95(0.05)
53.9 S	24.5 E	19.36(0.06)	18.91(0.06)	18.75(0.05)
50.8 S	62.8 E	16.83(0.06)	16.44(0.05)	16.24(0.05)
65.9 S	49.4 E	16.27(0.06)	15.83(0.05)	15.59(0.05)

<sup>a</sup> Offsets in arcseconds measured from the supernova.<sup>b</sup> Numbers in parentheses are uncertainties.